Characteristic temperature dependence of the $4f$ occupancy in the Kondo system $CeSi_2$

C. Grazioli, Z. Hu, M. Knupfer, G. Graw, G. Behr, M. S. Golden, and J. Fink
Institute for Solid State and Materials Research Dresden, P.O. Box 270016, D-01171 Dresden, Germany

H. Giefers and G. Wortmann
Fachbereich 6-Physik, Universität Paderborn, D-33095 Paderborn, Germany

K. Attenkofer
HASYLAB at DESY, Notkestrasse 85, D-22603 Hamburg, Germany
(Received 27 June 2000; published 27 February 2001)

We present a Ce-L_3 x-ray absorption spectroscopic study (XAS) of $CeSi_2$ at different temperatures. The extracted Ce $4f$ occupancy shows a strong dependence upon temperature that qualitatively agrees with theoretical expectations based on the single-impurity Anderson model. We additionally discuss the reliability of L_3 XAS performed on nearly trivalent rare-earth compounds in comparison with other high-energy spectroscopy techniques.

DOI: 10.1103/PhysRevB.63.115107 PACS number(s): 78.70.Dm, 71.27.+a

I. INTRODUCTION

The properties of rare-earth Kondo systems reflect those of the $4f$ states, characterized by strong correlation and hybridization with the band states. One of the central parameters in the description of this class of compounds is the f occupancy, n_f, and its dependence upon temperature.[1] Usually the contribution of the $4f$ states to the bonding is negligible, but in several rare-earth compounds they possess such a small $4f$ conduction band promotional energy that their hybridization with valence states can result in an intermediate-valent phase. In nearly trivalent Ce compounds, for instance, the single $4f$ electron is located below the Fermi level and its hybridization with the band states can lead to formation of a singlet state at low temperatures.

High-energy spectroscopies such as x-ray absorption, photoemission and resonant photoemission (abbreviated as XAS, PES, and RPES) are very useful to obtain microscopic information on the $4f$ hybridization in the ground state of Kondo systems.[2–4] Nevertheless some of their features and the related data interpretation are still not well understood and continue to be a matter of considerable debate. In particular, there has been a lively discussion in the past few years as to whether the results from PES support the Kondo scenario based on interpretation of the data within the single-impurity Anderson model (SIAM) or not,[5–7] despite the fact that the SIAM is very successful for rationalizing thermodynamic and transport properties of Kondo systems in general.

In the light of the great importance of the applicability of the SIAM to explain the microscopic features of Kondo systems, we have carried out a systematic XAS study at the L_3 absorption edge of $CeSi_2$, a simple standard Kondo system, in order to extract quantitatively the Ce $4f$ occupancy n_f as a function of temperature. Ce-L_3 XAS has been chosen because it is a powerful probe to extract the distribution of valence electrons in rare-earth and Kondo systems, and its interpretation is well understood.[8–11] In particular, a lot of effort has been expended to study the final state features with the aim of determining the ground state properties. The advantages of Ce-$L_{2,3}$ XAS in comparison to other high-energy spectroscopies are (1) the $\underline{c}4f^0 5d^*$-related final state peak ($\underline{c}$ denotes a core hole) has large spectral weight; therefore Ce-L_3 XAS is highly sensitive to the $4f$ occupancy;[9] (2) the mixture of the $\underline{c}4f^0 5d^*$ configuration with the $\underline{c}4f^n 5d^*$ ($n>0$) configurations is relatively low as compared to the corresponding peak in Ce$M_{4,5}$ XAS;[12,13] (3) XAS at the $L_{2,3}$ edge is performed using hard x rays ($E \sim 5720$ eV), and is thus fully bulk sensitive and free from possible surface-related effects in contrast to the high surface sensitivity of PES studies.

In an impurity picture, each property of a Kondo system is a universal function of the temperature scaled by T_K, the Kondo temperature.[1] Therefore n_f is also expected to scale with the T_K. In this contribution we show that in bulk single crystalline $CeSi_2$ n_f exhibits a clear temperature scaling that supports the description of Kondo systems within the SIAM, and we present a quantitative analysis of n_f as a function of temperature for this system.

II. EXPERIMENT

$CeSi_2$ with a tetragonal α-$ThSi_2$ structure is the silicide with the highest melting temperature within the binary Ce-Si system. The compound forms congruently from a melt with a composition of 35 mole % Ce, thus differing from the stoichiometric composition.[14] By differential thermal analysis (DTA) the melting temperature of the compound was measured to be 1703 °C, which is about 80 K above the melting point reported previously.[14] Polycrystalline feed rods were prepared from bulk pieces of Ce and silicon of purity 99.9% or better, which were arc-melted several times to achieve homogeneous samples. After remelting in a Hukin-type cold crucible rods of 6 mm in diameter and 55 mm in length were cast from a rf levitated melt.[15] Bulk single crystals of $CeSi_2$ were grown by the rf floating zone method (250 kHz, 30 kW) from the polycrystalline feed rods (for details of the growth facility see Ref. 16). The single crystals were

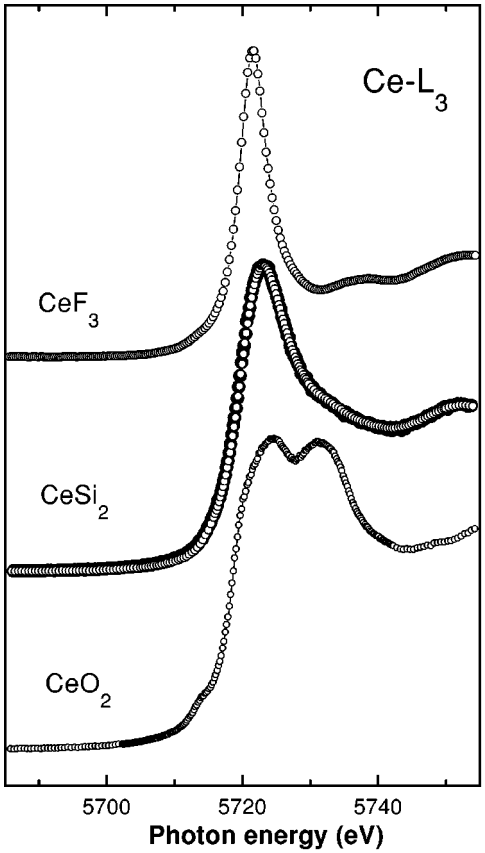

FIG. 1. Ce-L_3 XAS of $CeSi_2$ at room temperature together with the standard compounds CeF_3 (Ce^{3+}) and CeO_2 (Ce^{4+}). As a check for possible contaminations in $CeSi_2$ we superimposed the spectra of the $CeSi_2$ adsorber (open circles) and an unpowdered single crystal (filled circles): it is apparent that no difference is detectable.

then cut using a diamond-coated wire, and their crystal structure was checked using x-ray diffraction.

The Ce-L_3 XAS experiments were performed at the EXAFS-II and A1 beam lines in HASYLAB in the transmission geometry with the help of three ionization chambers in series for the sample and a reference. Since in the energy range of the Ce-L_3 edge the sample thickness should not exceed a few micrometers, we finely powdered the single crystal in a glove box and mixed it with paraffin in order to protect it from air. Measuring the powdered single crystal in transmission has the advantage of having no polarization-dependent effects and no self-absorption distortion. The measurements were recorded in a few days after the sample preparation, and we detected no appreciable change due to oxidation. In this way, the sample, being prepared starting from a high-quality single crystal, was free from any kind of intrinsic contamination like foreign phases. We also prepared homogeneous absorbers of polycrystalline CeF_3 and CeO_2 as reference compounds.

III. RESULTS

Figure 1 shows the Ce-L_3 spectrum of $CeSi_2$ at room temperature together with those of CeF_3 and CeO_2 as trivalent and tetravalent reference compounds, respectively. XAS at the rare-earth L_3 threshold is due to $2p_{3/2} \rightarrow 5d$ excitations and can be separated into continuumlike edges and atomiclike transitions (white lines, WL). CeF_3 exhibits only a single WL, which is attributed to the $\underline{2p}4f^1 5d^*$ final state, while CeO_2 shows a double-peaked structure originating mainly from mixed $\underline{2p}4f^0 5d^*$ and $\underline{2p}4f^1 5d^*$ final states ($\underline{2p}$ denotes the $2p$ core hole).[17–19] There is, in addition, also a contribution from $\underline{2p}4f^2 5d^*$, mixed mostly with the $\underline{2p}4f^0 5d^*$ final state, but it is smaller than the other two, reflecting the fact that the contribution of $4f^2$ in the ground state is small because of the $4f$ electron-electron repulsion U_{ff} (about 10 eV). The contribution from higher 4f occupancies is negligible. Since the low- and high-energy peaks have dominantly $|f^1\rangle$ and $|f^0\rangle$ character,[18] respectively, they are commonly labeled $|f^1\rangle$ and $|f^0\rangle$ for classification purposes.

The $CeSi_2$ spectrum consists of a main WL at 5722 eV, which corresponds to the $|f^1\rangle$ peak in CeF_3 and CeO_2. At about 10 eV higher energy a small satellite is visible as has been already reported previously,[20] which corresponds to the $|f^0\rangle$ peak in CeO_2. The presence of the high-energy satellite indicates a small presence of $4f^0$ in the ground state, i.e., the Ce valence in $CeSi_2$ is somewhat greater than 3. Since it can be argued that the powdering and the paraffin could introduce external contamination, we compared a spectrum taken in transmission on our absorber with one recorded in fluorescence on an unpowdered single crystal: no tetravalent impurities (which are a clear sign of contamination) were detected in the former (see Fig. 1). In fact, if the sample would have become oxidized, this would lead to a stronger $|f^0\rangle$ peak due to the presence of CeO_2. From Fig. 1 it is clear that no difference is detectable, i.e., the tetravalent contribution in $CeSi_2$ spectra does not arise from tetravalent CeO_2 impurities due to oxidation but is intrinsic.

In Fig. 2 we show the Ce-L_3 spectrum for 300 K, 100 K, and 10 K. Cooling the $CeSi_2$ sample has the effect of increasing the satellite intensity with respect to the main line. We attribute this effect to a decrease of the $4f$ occupancy at lower temperatures.

A qualitative analysis of the Ce valence, v, can be performed based upon the simple intensity ratio between the satellite and main peak:

$$v = 3 + \frac{I_{Satellite}}{I_{Main} + I_{Satellite}}. \qquad (1)$$

This method is equal to the assumption that the lower-energy peak in the Ce-L_3 XAS corresponds to a pure $4f^1$ configuration and the higher-energy peak to a pure $4f^0$ configuration in the ground state (see, e.g., Ref. 21). The change of the $4f$ occupancy with temperature obtained using this method is shown in Fig. 3 as open squares. From Fig. 3 it is immediately clear that the $4f$ occupancy in $CeSi_2$ exhibits a characteristic temperature dependence. Below about 40 K it is constant and increases significantly above this temperature.

In order to extract the $4f$ occupation more precisely, we make use of a simplified version of the Anderson impurity

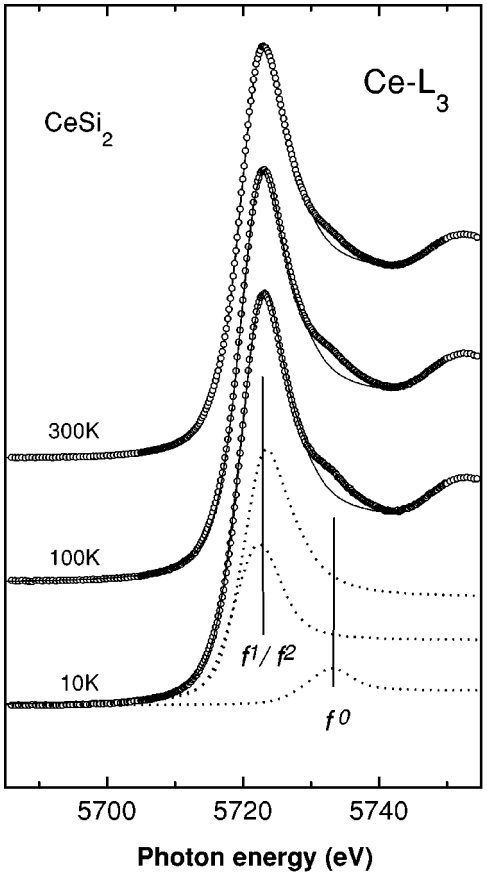

FIG. 2. Ce-L_3 XAS of $CeSi_2$ at 300 K, 100 K, and 10 K. A fit of the main peak is additionally shown (solid line) to underline the change in intensity of the $\underline{2p}4f^05d^*$ related final state feature. The dashed lines represent the decomposition into the three final states for the spectrum at 10 K as described in the text.

model as introduced by Imer and Willoud[22] in the zero-bandwidth limit, based upon the fact that the intra-atomic multiplet interactions are negligible in Ce-L_3 XAS spectra.[9] In this model the Hamiltonian and wave functions are written as

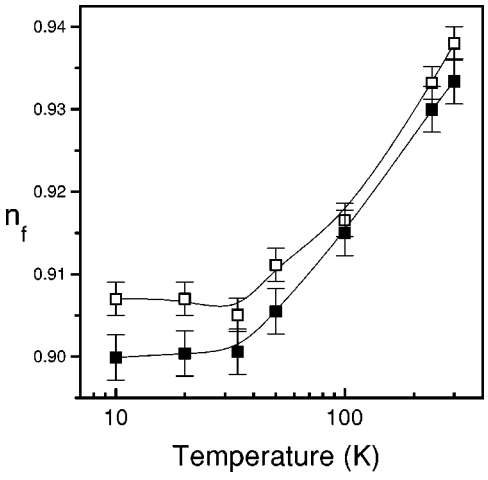

FIG. 3. (a) Ce $4f$ occupancy, extracted from Ce-L_3 XAS versus T obtained using Eq. (1) (open squares) and Eqs. (2)–(6) (solid squares). The error bars are the standard deviation of the two fits.

TABLE I. The parameter set used in Eqs. (2)–(6); all values are given in eV. The values of U_{ff}, U_{cf}, and U_{fd} are slightly smaller than in CeO_2 (Ref. 19) as expected from the better screening in the metallic systems. V has been adjusted in order to fit the experimental data while Δ has been kept constant.

$V(T=0)$	$V(T=300)$	Δ	U_{ff}	U_{fc}	U_{fd}
0.92	0.6	-1.75	8.5	12.0	4.5

$$\begin{pmatrix} 0 & V & 0 \\ V & U_1 & \sqrt{2}V \\ 0 & \sqrt{2}V & U_2 \end{pmatrix} \begin{pmatrix} u_k \\ v_k \\ w_k \end{pmatrix} = E_k \begin{pmatrix} u_k \\ v_k \\ w_k \end{pmatrix}, \tag{2}$$

where

$$\Psi_g = u_0|f^0\rangle + v_0|f^1\rangle + w_0|f^2\rangle \tag{3}$$

for the ground state, and

$$\Psi_f = u_f|\underline{2p}\,4f^05d^*\rangle + v_f|\underline{2p}\,4f^15d^*\rangle + w_f|\underline{2p}\,4f^25d^*\rangle \tag{4}$$

for the final states. $U_1=\Delta$ and $U_2=2\Delta+U_{ff}$ for the initial state, while $U_1=\Delta-U_{cf}+U_{fd}$ and $U_2=2U_1+U_{ff}$ for the final states. Δ denotes the charge transfer energy between the $4f$ and the conduction band states; V is the hybridization between the f level and the band states. U_{ff}, U_{cf}, and U_{fd} are the $4f$-$4f$, the core-hole–$4f$ and the $4f$-$5d$ Coulomb interactions, respectively (their values are summarized in Table I). The spectral intensity of each eigenvalue E_f is given by

$$I(E_f) = (u_0u_f + v_0v_f + w_0w_f)^2. \tag{5}$$

At the bottom of Fig. 2 we have plotted a decomposition of the absorption edge of $CeSi_2$ into the three final states as represented by Eq. (2) for the spectrum taken at 10 K. The high-energy component is the f^0 final state, while the other two are mixed f^1 and f^2 final states. Each final state itself was represented by a Lorentzian function, with an arctanlike step function describing the edge jump. To reduce the number of free parameters to a minimum, the energy separation between the Lorentzian and the arctangent step function as well as their intensity ratio were kept equal for all final state components (for details see Refs. 8 and 9). Finally, the data were broadened by a Gaussian function of width 1.9 eV to account for the finite experimental energy resolution. The initial trial parameter set was estimated from $3d$ x-ray photoemission spectroscopy (XPS) data of $CeSi_2$. Subsequently, the values of U_{ff} and U_{cf} were kept fixed at these values, while Δ, V, and $(U_{cf}-U_{fd})$ were varied in order to achieve an optimal fit to the XAS data. The values of Δ and U_{fd} were constrained to be independent of temperature, leaving V as the only free variable to describe the temperature dependence of the spectra. The values of U_{ff} and U_{cf} that we estimated from $3d$ XPS are representative of the bulk since they remain essentially unchanged at the surface.[23] The fit parameters are summarized in Table I.

Using this fitting procedure we can now easily extract the average $4f$ occupancy in the ground state for all temperatures as

$$n_f = |v_0|^2 + 2|w_0|^2. \quad (6)$$

In Fig. 3 we have plotted the temperature dependence of the $4f$ occupation number, n_f, deduced using this procedure, as filled squares. Again, its value is almost constant at $n_f = 0.9$ below 40 K, then it increases monotonically, reflecting a decrease in $4f$ hybridization or increase of $4f$ localization.

Comparing $n_f(T)$ extracted with the two methods described above, we notice that Eq. (1) gives an acceptable temperature dependence of the $4f$ occupancy, although the absolute values obtained are not correct. At room temperature, Eq. (1) gives results close to the quantitative analysis described above, while at low temperatures it is markedly different. The small difference at room temperature is due to the fact that, for such low hybridizations, the satellite has more than 99% $4f^0$ character; thus the situation corresponds approximately to Eq. (1), while at low temperatures the mixture between $4f^0$ and $4f^1$ increases. The increase in the configurational mixture is small but significant and influences the result of Eq. (1). This shows that, in general, the $4f^1$ contribution is overestimated by the application of Eq. (1).

Returning to the results of Fig. 3, we have found that the $4f$ occupancy, n_f, in the classical Kondo system $CeSi_2$ increases with temperature above about 40 K, while it is constant below this temperature. This is exactly what one would expect within the impurity model and shows that this model is able to provide a good microscopic understanding of such Kondo systems although the $4f$ states are not single impurities. We attribute the success of the impurity model to the fact that the $4f$ states are spatially separated enough to inhibit a direct interaction between them. Moreover, from our results one can derive an estimate of the Kondo temperature, T_K, by a comparison of the temperature behavior of n_f as shown in Fig. 3 and theoretical expectations based upon the Anderson model.[1] This would lead to a relatively high T_K of roughly 100–140 K, which is larger than the value extracted from PES [$T_K \sim 35$ K (Ref. 2)] but closer to the values derived from magnetization and specific heat measurements [$T_K \sim 69-132$ K (Ref. 24)]. One should take care that an estimation of T_K would not be realistic within our simple calculation.[22] This is due to the fact that the very low-energy excitations (i.e., the spin excitations) are not well accounted for in the limit of infinitely narrow bandwidth.

From the data plotted in Fig. 3 (filled squares) we obtain $n_f(T=0) = 0.9$, which is much smaller than 0.97 extracted from PES data.[2] This strong difference between the results from PES and XAS can be rationalized considering that at the surface of several Ce compounds the average valence is significantly altered,[25] thus leading to an almost trivalent surface. This is true also for $CeSi_2$ as extracted from Ce $3d$ XPS data (not shown) and means that $n_f(T=0)$ is overestimated with surface sensitive measurements while the corresponding Kondo temperature is underestimated.

The influence of the surface might also explain why it has been deduced that the PES spectral features show no temperature scaling with T_K and that their temperature dependence can be easily explained by means of a conventional phonon broadening. In the review in Ref. 26, in particular, the authors argue that n_f does not scale with T_K and discuss the disagreement between PES and XAS by taking into consideration extensively the hypothetical existence of a subsurface layer that is different from both the surface and the bulk, but leaving the problem substantially unresolved. The point we wish to make here is that although PES is a powerful probe of such correlated electron systems (further argumented by the improvement in resolution attained in the last few years), the surface sensitivity intrinsic to the technique can lead to considerable errors if one restricts the experimental interpretation to data from a single technique.

IV. SUMMARY

In summary, we have used bulk sensitive Ce-L_3 XAS to measure a powdered single crystal of $CeSi_2$ and we have shown that the Ce $4f$ occupancy, n_f, shows a temperature-dependent behavior that is in good agreement with expectations from the single Anderson impurity model. The discrepancy between our results from x-ray absorption spectroscopy and those obtained using photoemission spectroscopy most probably arise from the surface sensitivity of the latter, i.e., the surface of various Kondo systems can exhibit a physical behavior different from the bulk.

ACKNOWLEDGMENTS

This work was supported by the Deutsche Forschungsgemeinschaft (DFG) within the SFB 463 *''Seltenerd-Übergangsmetallverbindungen: Struktur, Magnetismus und Transport.''* Z.H. also acknowledges the *Graduiertenkolleg ''Struktur und Korrelationseffekte in Festkörpern''* at the TU Dresden. C.G. is grateful to C. Schüssler-Langeheine for the help in writing the fit routines and to C. Laubschat for valuable discussions.

[1] N. E. Bickers, D. L. Cox, and J. W. Wilkins, Phys. Rev. B **36**, 2036 (1987).

[2] F. Patthey, J.-M. Imer, W.-D. Schneider, H. Beck, Y. Baer, and B. Delley, Phys. Rev. B **42**, 8864 (1990).

[3] J. M. Lawrence, A. J. Arko, J. J. Joyce, R. I. R. Blyth, R. J. Bartlett, P. C. Canfield, Z. Fisk, and P. S. Riseborough, Phys. Rev. B **47**, 15 460 (1993).

[4] D. Malterre, M. Grioni, and Y. Baer, Adv. Phys. **45**, 299 (1996).

[5] M. Garnier, K. Breuer, D. Purdie, M. Hengsberger, Y. Baer, and B. Delley, Phys. Rev. Lett. **78**, 4127 (1997).

[6] A. J. Arko and J. J. Joyce, Phys. Rev. Lett. **81**, 1348 (1998).

[7] M. Garnier, D. Purdie, K. Breuer, M. Hengsberger, Y. Baer, and

B. Delley, Phys. Rev. Lett. **81**, 1349 (1998).
[8] Z. Hu, S. Bertram, and G. Kaindl, Phys. Rev. B **49**, 39 (1994).
[9] Z. Hu, E.-J. Cho, G. Kaindl, and B. G. Müller, Phys. Rev. B **51**, 7514 (1995).
[10] D. Malterre, Phys. Rev. B **43**, 1391 (1991).
[11] G. Kaindl, G. Schmiester, E. V. Sampathkumaran, and P. Wachter, Phys. Rev. B **38**, 10 174 (1988).
[12] H. Ogasawara, A. Kotani, and K. Okada, Phys. Rev. B **43**, 854 (1991).
[13] T. Jo and A. Kotani, J. Phys. Soc. Jpn. **57**, 2288 (1988).
[14] *Binary Alloy Phase Diagrams*, edited by T. B. Massalski, H. Okamoto, P. R. Subramanian, and L. Kaprazak, 2nd ed. (ASM International, Metals Park, OH, 1992), Vol. 3.
[15] O. Thomas, J. P. Senateur, R. Modar, O. Laborde, and E. Rosender, Solid State Commun. **55**, 629 (1985).
[16] G. Behr, W. Löser, G. Graw, H. Bitterlich, J. Freudenberger, J. Fink, and L. Schultz, J. Cryst. Growth **198-199**, 642 (1999).
[17] G. Kaindl, G. K. Wertheim, G. Schmiester, and E. V. Sampathkumaran, Phys. Rev. Lett. **58**, 606 (1987).
[18] A. Bianconi, A. Marcelli, H. Dexpert, R. Karnatak, A. Kotani, T. Jo, and J. Petiau, Phys. Rev. B **35**, 806 (1987).
[19] T. Jo and A. Kotani, Solid State Commun. **54**, 451 (1985).
[20] J. M. Lawrence, M. L. den Boer, R. D. Parks, and J. L. Smith, Phys. Rev. B **29**, 568 (1984).
[21] J. Röhler, in *Handbook on the Physics and Chemistry of the Rare-Earths*, edited by K. A. Gschneider Jr., L. R. Eyring and S. Hüfner (Elsevier, Amsterdam, 1999), Vol. 10, pp. 453–546.
[22] J. M. Imer and E. Willoud, Z. Phys. B: Condens. Matter **66**, 153 (1987).
[23] L. Duò, P. Vavassori, L. Braicovich, M. Grioni, D. Malterre, Y. Baer, and G. L. Olcese, Phys. Rev. B **53**, 7030 (1996).
[24] Yashima, H. Mori, T. Satoh, and K. Kohn, Solid State Commun. **43**, 193 (1982).
[25] C. Laubschat, E. Weschke, C. Holtz, M. Domke, O. Strebel, and G. Kaindl, Phys. Rev. Lett. **65**, 1639 (1990).
[26] A. J. Arko and P. S. Riseborough, in *Handbook on the Physics and Chemistry of the Rare-Earths*, edited by K. A. Gschneider Jr., L. R. Eyring, and S. Hüfner (Elsevier, Amsterdam, 1999), Vol. 26, pp. 265-382.